COMPARISON BETWEEN PREDICTED AND MEASURED BLACKOUT BOUNDARIES FOR EARTH ENTRY OF APOLLO[+]

By Michael G. Dunn

Cornell Aeronautical Laboratory, Inc.
Buffalo, New York 14221

ABSTRACT

A semiempirical technique has been developed to calculate the non-equilibrium flow electron-density and collision-frequency distributions in the plasma surrounding an Apollo vehicle during earth-atmosphere entry. Utilizing the results of these calculations, the communication-blackout boundaries were constructed for a carried frequency of 2.287 GHz for an entry velocity range of 14,000 to 35,000 ft/sec. For any arbitrary entry velocity in this range, the altitude uncertainty band is ± 5000 ft. The predicted boundaries are compared to in-flight data gathered by the NASA[*] for Apollo 4, 6, 7, 8, and 10. The agreement between the predicted and measured blackout boundaries is reasonably good.

INTRODUCTION

Prior to the initiation of the Apollo program, experience with the Mercury and Gemini earth-orbiting space vehicles had indicated that communications with the craft at customary radio frequencies was impossible during a significant portion of the entry trajectory as a result of free electrons in the surrounding plasma. The increased entry velocity associated with Apollo upon return from lunar missions implied considerably higher electron densities than previously experienced and thus an extended period of time over which signal transmissions would be significantly degraded (blackout). For the purposes of the flight data communications blackout will be defined as that point in the trajectory at which the received signal becomes equal to the

---

[+]This paper is based on research sponsored by the NASA, Goddard Space Flight Center, under Contract NAS5-9978. Many people at Cornell Aeronautical Laboratory have contributed to this work. A complete list of credits is given in CAL Report No. AI-2187-A-17.

[*]These data were recently supplied to the author by Dr. Richard Lehnert, National Aeronautics and Space Administration, Goddard Space Flight Center, Greenbelt, Maryland.

receiver threshold. The most desirable solution to this difficulty would be to reduce the electron density to an acceptable level. It soon became apparent that alleviation might not be practical and therefore an accurate prediction of the trajectory position of onset and termination of signal degradation was the next best solution. It was this latter interest that motivated the research reported in this paper.

The Apollo vehicle is very blunt and enters the earth atmosphere at a large (approximately 20°) angle of attack. Early in the program it was determined that if accurate estimates of the communication blackout boundaries were to be made, then significantly more information about chemical kinetics, flow-field predictions, separated flow, and ablation products would be required. Each of these areas was investigated in some detail and the results are summarized in Reference 1. The material presented in this paper is a much condensed version of that outlined in Reference 1.

As an initial step in this program streamline locations and pressure distributions in the asymmetric inviscid flow field were obtained from the time-dependent solution of Bohachevsky and Mates.[2] This information was then used[3] to perform nonequilibrium chemical kinetics calculations by means of a streamtube technique. The results of this effort were helpful in determining the important chemical reactions and for which of the reactions rate coefficient data were needed. With this information, an experimental program was initiated to measure the important reaction-rate coefficients under laboratory conditions.

The inviscid flow-field calculation noted above was a good starting point, but it was clear that at altitudes greater than approximately 250,000 ft the thin boundary-layer approximation begins to break down for flow around the Apollo body and thus could not be used. The influence of the transport properties is spread across the shock layer, and even the shock wave itself may not be thin compared to the stand-off distance. Solutions for the gasdynamic variables and chemical compositions were therefore obtained[4-6] for these low-density flows using an approximate analysis based on an integral method.

The experimentally determined reaction-rate coefficient data for the electron-depletion reactions and the theoretical analyses developed were integrated, and calculations were performed at selected trajectory points in order to arrive at a prediction of the communication-blackout boundaries for the Apollo entry upon return from lunar missions. The entry trajectory is such that two different flow-field regimes were necessarily considered in order to calculate the gasdynamic parameters and chemical compositions. During the early portion (high altitude) the flow field is viscous. At lower altitudes, below about 250,000 ft, the thin boundary-layer assumption becomes valid and inviscid-flow calculations are appropriate for calculation of the plasma properties.

In the remainder of this paper the calculations performed to obtain the predicted boundaries will be briefly described. Comparison will be made between the predictions and flight data from Apollo 4, 6, 7, 8, and 10 flights.

CONSTRUCTION OF INVISCID FLOW FIELD

The calculation technique of Reference 2 was not used in the later stages of this research because of the wealth of experimental data that became available. It was more realistic and less expensive to use these data to construct the shock envelope and flow field in the pitch plane for an Apollo vehicle at a 20 degree angle of attack. The flow field was divided into the subsonic-transonic forebody region and the supersonic afterbody region. Ablation effects were not included in these calculations because they were previously considered by Huber[7]. His results are compared to the pure-air chemistry blackout boundaries later in the paper.

The shock envelope in the forebody region was determined using the empirical correlation functions of Kaattari[8] for a twenty degree angle of attack and a normal-shock density ratio of sixteen. The shock-wave shape in the vicinity of the round (toroid) windward corner was also determined by the procedure suggested in Reference 8.

In order to simplify the supersonic flow-field calculations, a single family of characteristics was used to predict the flow expansion around the rounded windward and leeward corners of the body. The pressure and flow inclination angle are constant along each characteristic. Since the corner-region expansion fan is assumed to be isentropic, the procedure does not take into account the entropy gradients due to the curved shock wave. Also, since only one family of characteristics is considered the reflections from the shock wave and streamlines are neglected; this should not have a large influence on the results since these reflections tend to cancel each other.

The experimentally determined surface-pressure distribution for a 0.05-scale model of the Apollo vehicle was used to determine the leading and trailing characteristics of the expansion fan around the rounded leeward and windward corners in the pitch plane. The expansion fan was constructed graphically utilizing the local flow inclination angle of the Apollo vehicle surface and tabulated Prandtl-Meyer functions[9] for $\gamma = 1.4$. The pressure ratio P_2 / P_5 is constant along each characteristic since the expansion is assumed to be isentropic. The local pressure along the characteristic is P_2 and the stagnation pressure behind the shock is P_5 .

The flow inclination angle computed from the conservation equations for a given pressure ratio P_2 / P_∞ was not the same as the flow inclination angle at the body surface along a given characteristic because of entropy gradients produced by the curved shock which will alter the location of the characteristics. To account for the entropy gradients in a simple manner, it was assumed that the flow deflection angle varied linearly from the flow angle at the surface to the flow angle imposed by the conservation equations at the shock wave along each characteristic. Selected streamlines can then be constructed graphically since the local flow inclination angles are now known. The locations of the streamlines in the subsonic forebody region were determined by enforcing the conservation of mass for axisymmetric flow. The product $\rho \vec{q}$ of the density and velocity vector was assumed to be constant along normals to the forebody surface.

Figure 1 illustrates the location of nine streamlines that were constructed in the plane of symmetry. The oblique-shock calculations indicated that the shock-wave envelope is independent (within 6%) of the flight conditions considered here. In addition to the above streamlines, two streamlines were assumed to originate at the stagnation point and to expand around the body with a pressure distribution that matches the experimentally observed surface-pressure distribution. The leeward side streamline then was assumed to depart from the body surface in the corner region with a flow-inclination angle consistent with the trailing characteristic as determined by the afterbody pressure. This streamline was called the separation streamline since it did not follow the afterbody surface. The windward streamline almost follows the afterbody surface and indicates that a thin, viscous boundary layer exists along the windward side of the vehicle with no apparent separation region.

Having determined the shock shape and the location of several streamlines within the shock layer, the initial conditions on the streamlines just behind the shock wave were calculated for frozen composition and vibrational equilibrium. The nonequilibrium electron-density and collision-frequency histories were then calculated[10] utilizing the initial conditions and the pressure distribution along the streamlines. The oblique shock-wave solutions provided the initial conditions for each streamline with the exception of the windward- and leeward-surface streamlines which used stagnation conditions determined from normal-shock solutions.

CHEMICAL KINETICS CALCULATIONS

The inviscid flow field briefly outlined above was used to obtain estimates of the electron-density and collision-frequency distributions in the plasma surrounding the Apollo vehicle. Trajectory points for which calculations were performed are given in Table 1 below. Note that for two of the last three trajectory points given in this table, it is necessary to account for viscous-flow influences. This correction has been made and is discussed later.

TABLE 1

TRAJECTORY POINTS FOR WHICH INVISCID FLOW-FIELD CALCULATIONS WERE PERFORMED

VELOCITY, ft/sec	ALTITUDE, ft
10,000	150,000
14,000	120,000
16,000	180,000
16,000	210,000
21,000	240,000
21,000	250,000
26,000	280,000
32,000	320,000
34,000	220,000

Species-distribution plots similar to those shown in Figures 2 and 3 (34,000 ft/sec at 220,000 ft) were obtained for each trajectory point of Table 1 and were used in constructing the blackout bounds presented in Figure 4 for 2.287 GHz communication. The system of chemical reactions used here was the same as that used in Reference 3 with the major exception that the rate coefficients for the electron depletion reactions $NO^+ + e^- \longrightarrow N + O$, $N_2^+ + e^- \longrightarrow N + N$ and $O_2^+ + e^- \longrightarrow O + O$ were those measured[11-13] as part of this research. In obtaining the blackout boundaries, the decision was made to define blackout on the basis of the critical electron density. Rays were then drawn from the antenna location through the plasma and across the shock envelope. If the local electron density along the particular ray exceeded the critical electron density (6.5×10^{10} e^-/cm^3 for 2.287 GHz communications), then the signal strength was assumed sufficiently degraded so as to be not useful. It was further assumed that the acute included angle between the shock envelope and the ray must be greater than 5° before communications would be possible, even if the local electron density along the ray did not exceed critical.

Figure 4 illustrates typical rays drawn from the S-band antenna location through the leeward-side plasma. For this particular flight condition, the electron density along ray A exceeded critical n_e for a significant portion of the path making communications impossible. Along ray B the number density was again significantly greater than critical for much of the propagation path. However, along ray C the number density is near but almost always less than critical, making communications marginal. Ray C crosses the shock envelope at approximately 12.5°, suggesting that within the constraints of our assumptions this trajectory point would be classified as marginal communications.

No rays were drawn through the windward-side plasma for the trajectory condition of Figure 4 because the electron-density profile for this condition was such as to suggest that the exit path for the E-M wave could not be a direct one. The conclusion should not be drawn, however, that communications through the leeward-side plasma was most likely for all trajectory points. For flight velocities greater than 21,000 ft/sec, the results suggested that the best chances for communications were in fact through the leeward-side plasma. However, for lower velocities and lower altitudes the communications through the windward-side plasma was more likely. This effect is a result of the nonequilibrium chemistry of the reactions involving charged particles and the manner in which they proceed in the respective expansion environment (leeward vs. windward).

Figure 5 presents the prediction (for pure-air flow) of the communication-blackout boundaries for 2.287 GHz with an estimated uncertainty of approximately ± 5000 ft altitude. Each of the calculated trajectory points is noted on this plot as communications should not be degraded (⊡), marginal communications (⊙), and communications should be blacked out (△). It is emphasized that these are calculated points and not in-flight data points.

Also included on Figure 5 are the blackout bounds estimated by Huber[7] considering only ablation-product impurity ionization. At the higher velocities, it can be generally concluded that blackout boundary for Apollo

earth-atmosphere entry conditions is controlled by the pure-air chemistry. For flight velocities between 24,000 and 27,000 ft/sec and between 15,000 and 17,000 ft/sec, the ablation-controlled boundary falls within the lower altitude limit of the uncertainty band of the pure-air chemistry. It is thus suggested that in these flight regimes the pure-air and ablation chemistry are of equal importance. The early prediction of Lehnert and Rosenbaum[14] is also included on Figure 5 for comparison purposes. Their estimate differs from the current estimate for velocities greater than 21,000 ft/sec and for velocities lower than 16,000 ft/sec.

VISCOUS FLOW-FIELD CALCULATIONS

For altitudes greater than 250,000 ft, the thin boundary-layer approximation is no longer applicable for analyzing the flow around the Apollo body. The influence of the transport properties is spread across the shock layer, and even the shock wave itself may not be thin compared to the shock stand-off distance. Thus a new formulation is needed in analyzing the viscous flow around the body at low Reynolds numbers. The flow regimes of interest are the viscous layer, the incipient-merged layer, and part of the fully merged layer, viz., $O(\epsilon) \leq \epsilon K^2 \leq O(10^4)$. The term K^2 is the parameter defined by Cheng.[15] In particular, $K^2 = \left(\frac{\rho_\infty U_\infty a}{\mu_*}\right)\epsilon(T_*/T_0)$, $\epsilon = (\gamma-1)/2\gamma$, γ signifying the specific heat ratio, $\rho_\infty U_\infty$ the free-stream mass flux, a the nose radius of the body, T_0 the stagnation temperature, T_* and μ_* the reference temperature and viscosity, respectively. As $K^2 \longrightarrow \infty$, the flow approximates continuum, thin boundary-layer flow, while $K^2 \longrightarrow 0$ signifies free-molecule flow conditions. It has been found from the analysis[16] of the stagnation region that the term K^2 may still be used as a meaningful parameter delineating various flow regimes even for the case of mass injection. Thus the present viscous-flow analysis for an Apollo-type body is applicable at altitudes between approximately 250,000 ft and 400,000 ft.

The viscous flow-field analysis performed for the purposes of this contract began by considering the axisymmetric flow over the forebody region of an Apollo body with large mass injection at the wall due to ablation. The flow was in the incipient-merged-layer and the viscous-layer regimes. In these regimes, the Navier-Stokes equations may be used. The equations were simplified by assuming a very thin shock layer compared with the body radius.

The equations thus simplified are similar in form to the conventional boundary-layer equations with the important exceptions that the entire flow field is now viscous, instead of a very thin layer near the wall and that the normal pressure gradient may not be assumed negligible. The latter condition results because of the non-negligible momentum change in the direction normal to the body surface. An approximate analysis based on an integral method was formulated which takes into account large mass injection at the body surface as well as transport phenomena across the shock wave.

Results were initially obtained[4] for hypersonic, low Reynolds-number flow in the stagnation region of a blunt body at high altitudes by application of

the integral method. Significant influences of mass injection on the heat transfer, the "skin-friction," changes in flow conditions across the shock wave in the incipient-merged layer and the viscous-layer flow regimes were observed. Attention was subsequently concentrated on analyzing the viscous-flow phenomena downstream from the stagnation point in these flow regimes, and the results obtained from the stagnation-region analysis provided the initial conditions.

Solutions were then obtained[5] for the viscous, hypersonic shock layer in the forebody region of the Apollo body at high altitudes for the case of a non-reacting gas. This analysis yielded the streamline distributions within the viscous shock layer for various mass-injection rates. These results are particularly significant since they afford a means of assessing the importance of the viscous flow field on the plasma chemical kinetics. Solutions were obtained both with and without mass injection at the body surface. For the zero mass-injection case, the mass flowing in the viscous shock layer consists entirely of the free-stream mass entering through the shock wave; thus the stagnation streamline becomes the dividing streamline along the body and coincides with the body surface. When mass is now injected uniformly along the body at the surface, the layer in the immediate vicinity of the body surface consists of the injected mass and the dividing streamline is now pushed outward from the body. The thickening of the shock layer and the noticeably changed streamline patterns as a result of very large blowing was observed. Since the present analysis is based on a thin shock-layer assumption, it should be kept in mind that the justification of this assumption comes into question when the viscous shock layer becomes very thick (due to blowing) compared with the characteristic length of the body, which in this case is the body nose radius.

The viscous shock-layer work was continued in that an analysis of the chemical nonequilibrium flow in the forebody region of the Apollo body at high altitudes was formulated.[5] At the time, there were no previous analyses dealing with nonequilibrium flow around a blunt body that were directly applicable to the present problem. One analysis that should be mentioned is that performed by Lee and Zierten,[17] who considered the merged-layer ionization in the stagnation region of a blunt body without mass injection (ablation) at the body surface. These authors found that the inviscid theory overestimates the peak electron density by as much as two orders of magnitude.

Results were subsequently obtained for the binary-species nonequilibrium flow in the viscous shock layer for a fully catalytic surface. In analyzing the problem, the momentum and the energy equations and their solutions[5] were used as known inputs, under the assumption that the Lewis number is unity and effectively decoupling[14] the chemical considerations from the momentum and the energy considerations. An integral-method approach was used for the solution of the atom-concentration distributions along the body surface at various altitudes. In these calculations the only charged species were assumed to be e^- and NO^+.

The electron-density level was found[6] to be approximately two orders of magnitude below that predicted by an inviscid analysis. These results demonstrate a sizable influence of flow viscosity on the electron-density level at

high altitudes and that an inviscid analysis yields an upper-bound prediction of these levels. It is thus evident that analysis of the viscous shock layer was necessary in order to assess correctly the magnitudes of the electron-density levels existing in the forebody region of a blunt body at high altitudes. The results obtained for the viscous shock layer were incorporated in the communication-blackout boundaries presented in Figure 5.

COMPARISON BETWEEN PREDICTION AND FLIGHT DATA FOR 2.287 GHz COMMUNICATIONS

The in-flight communications blackout points reported here for Apollo 4 were taken directly from References 18, those for Apollo 6, 7, and 8 from Reference 19 and those for Apollo 10 from Reference 20. The measured signal strengths were obtained using the NASA instrumented aircraft 427 and 432, the Apollo range instrumented aircraft (ARIA), ground based Unified S-Band stations, and the reentry ships "Watertown," "Redstone" and "Huntsville." Typical signal strength data records and a detailed discussion of the instrumentation are presented in Reference 19. Figure 6 presents a comparison between the predicted communication-blackout boundaries and the in-flight data. Data points for Apollo 4, 8, and 10 were obtained for a velocity of approximately 35,000 ft/sec and are all in agreement as shown. The ARIA aircraft obtained data points for Apollo 4 for a freestream velocity of approximately 21,000 ft/sec at an altitude of approximately 240,000 ft which are in reasonable agreement with the prediction. The Apollo 6 blackout was obtained by both the NASA airplane and the "Watertown" and is also shown to be in agreement with the prediction. The ARIA 8 aircraft and the "Huntsville" both acquired signals from Apollo 10 for a velocity of approximately 16,000 ft/sec at an altitude of approximately 195,000 ft. These data points are approximately 20,000 ft above the predicted boundary.

The Apollo 7 results are somewhat more uncertain than the other measurements. In Reference 19 it is suggested that the high altitude loss of signal by NASA 427 aircraft, Merritt Island, and Grand Bahamas Island was anomalous because the ARIA 5 aircraft, which had a much different look angle, observed a signal strength decrease at the reported signal blackout, but continued to record signals beyond this time. It was concluded that the ARIA 5 aircraft lost signal at the trajectory point shown on Figure 6 but no positive evidence of plasma induced blackout was observed. The data for this flight exhibit significant disagreement with the predicted blackout boundaries. However, with the exception of this latter flight, the data appear to be in reasonable agreement with the predicted boundaries.

CONCLUSIONS

A map of the communication-blackout boundary for a carrier frequency of 2.287 GHz has been calculated for the earth-atmosphere entry of an Apollo

vehicle for the entry-velocity range 14,000 ft/sec to 35,000 ft/sec. The estimated altitude uncertainty for a given velocity in this range is $\pm$ 5000 ft. The comparison between predicted and measured blackout boundaries for Apollo 4, 6, 7, 8, and 10 is reasonably good.

REFERENCES

1. Dunn, M. G., "Predicted Communication Boundaries for Earth-Atmosphere Entry of the Apollo Vehicle," Final Report Contract No. NAS5-9978, Cornell Aeronautical Laboratory Report No. AI-2187-A-17, June 1969.

2. Bohachevsky, I. O. and Mates, R. E., "A Direct Method for Calculation of the Flow About an Axisymmetric Blunt Body at Angle of Attack," AIAA Journal, Vol. 4, No. 5, pp. 776-782 (1966).

3. Dunn, M. G., Daiber, J. W., Lordi, J. A. and Mates, R. E., "Estimates of Nonequilibrium Ionization Phenomena in the Inviscid Apollo Plasma Sheath," Cornell Aeronautical Laboratory Report No. AI-1972-A-1, September 1965.

4. Kang, S. W. and Dunn, M. G., "Integral Method for the Stagnation Region of a Hypersonic Viscous Shock Layer with Blowing," AIAA Journal, Vol. 6, No. 10, pp. 2031-2033, October 1968.

5. Kang, S. W., "Hypersonic, Low Reynolds-Number Flow over a Blunt Body with Mass Injection," AIAA Journal, Vol. 7, No. 8, pp. 1546-1552, August 1969.

6. Kang, S. W., "Nonequilibrium, Ionized, Hypersonic Flow over a Blunt Body at Low Reynolds Number," AIAA Journal, Vol. 8, No. 7, pp. 1263-1270, July 1970.

7. Huber, P. W., Addendum #2 to Minutes of the Eleventh Meeting of the Apollo Reentry Communications Blackout Working Group, July 18, 1967.

8. Kaattari, G. E., "Shock Envelopes of Blunt Bodies at Large Angles of Attack," NASA TN D-1980, December 1963.

9. Ames Research Staff, "Equations, Tables, and Charts for Compressible Flow," NACA Report 1135, 1953.

10. Lordi, J. A., Mates, R. E., and Mosselle, J. R., "Computer Program for the Numerical Solution of Nonequilibrium Expansions of Reacting Gas Mixtures," Cornell Aeronautical Laboratory Report AD-1689-A-6 (June 1965).

11. Dunn, M. G., and Lordi, J. A., "Measurement of Electron Temperature and Number Density in Shock-Tunnel Flows: Part II, $NO^+ + e^-$ Dissociative Recombination Rate in Air," to be published in AIAA Journal.

12. Dunn, M. G. and Lordi, J. A., "Measurement of $N_2^+ + e^-$ Dissociative Recombination in Expanding Nitrogen Flows," AIAA Journal, Vol. 8, No. 2, pp. 339-345, February 1970.

13. Dunn, M. G. and Lordi, J. A., "Measurement of $O_2^+ + e^-$ Dissociative Recombination in Expanding Oxygen Flows," AIAA Journal, Vol. 8, No. 4, pp. 614-618, April 1970.

14. Lehnert, R. and Rosenbaum, B., "Plasma Effects on Apollo Re-Entry Communications," NASA TN D-2732 (March 1965).

15. Cheng, H. K., "Hypersonic Shock-Layer Theory of the Stagnation Region at Low Reynolds Number," Proc. 1961 Heat Transfer and Fluid Mechanics Institute, Univ. of So. California, Stanford U. Press, pp. 161-175 (1961).

16. Chen, S. Y., Aroesty, J. and Mobley, R., "The Hypersonic Viscous Shock Layer with Mass Injection," Rand Corp. Memo RM 4631-PR (May 1966).

17. Lee, R. H. C. and Zierten, T. A., "Merged Layer Ionization in the Stagnation Region of a Blunt Body," 1967 Heat Transfer and Fluid Mechanics Inst., La Jolla, California, pp. 452-468 (June 1967).

18. Marini, J., "Apollo 4 Blackout Test Results, Mares Island Entry," NASA, Goddard Space Flight Center, X-551-68-419, November 1968.

19. Marini, J. W. and Hager, F. W., "Apollo 6, 7 and 8 Blackout Test Results," NASA, Goddard Space Flight Center, X-550-69-277, July 1969.

20. Private Communication with Dr. Richard Lehnert, National Aeronautics and Space Administration, Goddard Space Flight Center, July 2, 1970.

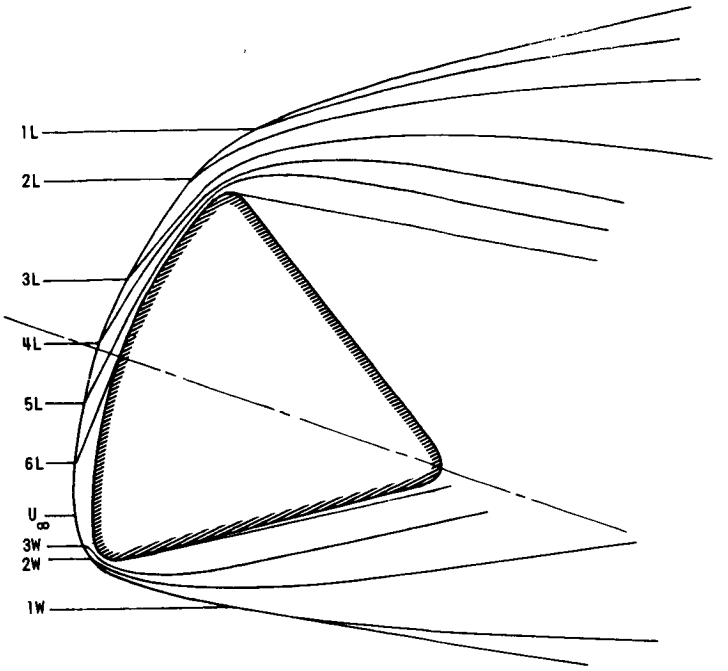

Figure 1.- Streamline pattern in the plane of symmetry.

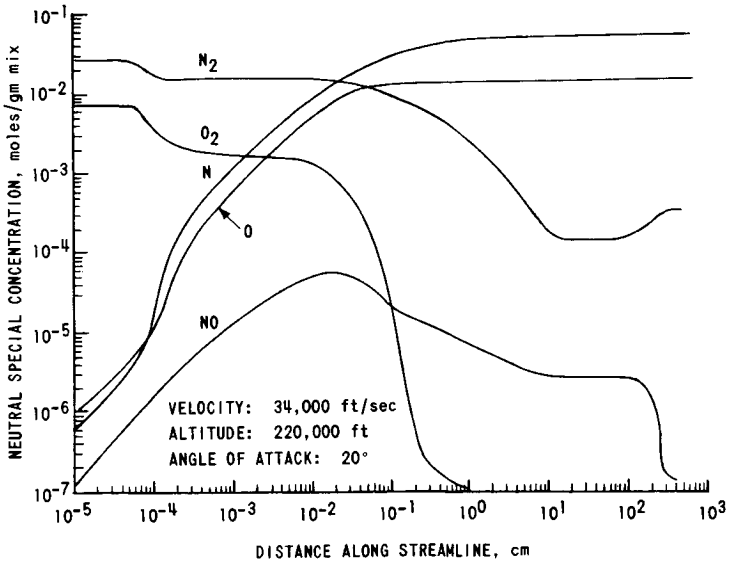

Figure 2.- Nonequilibrium species distribution along streamline 4L in plane of symmetry.

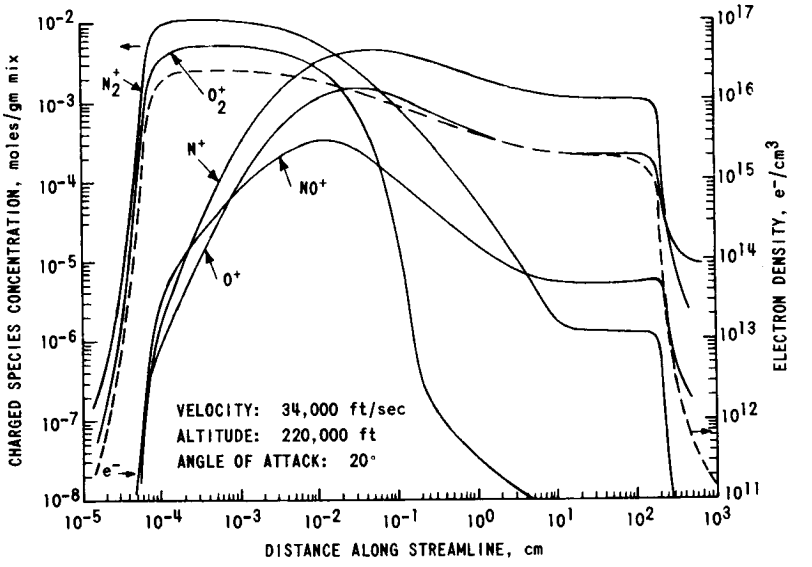

Figure 3.- Nonequilibrium species distribution along streamline 4L in plane of symmetry.

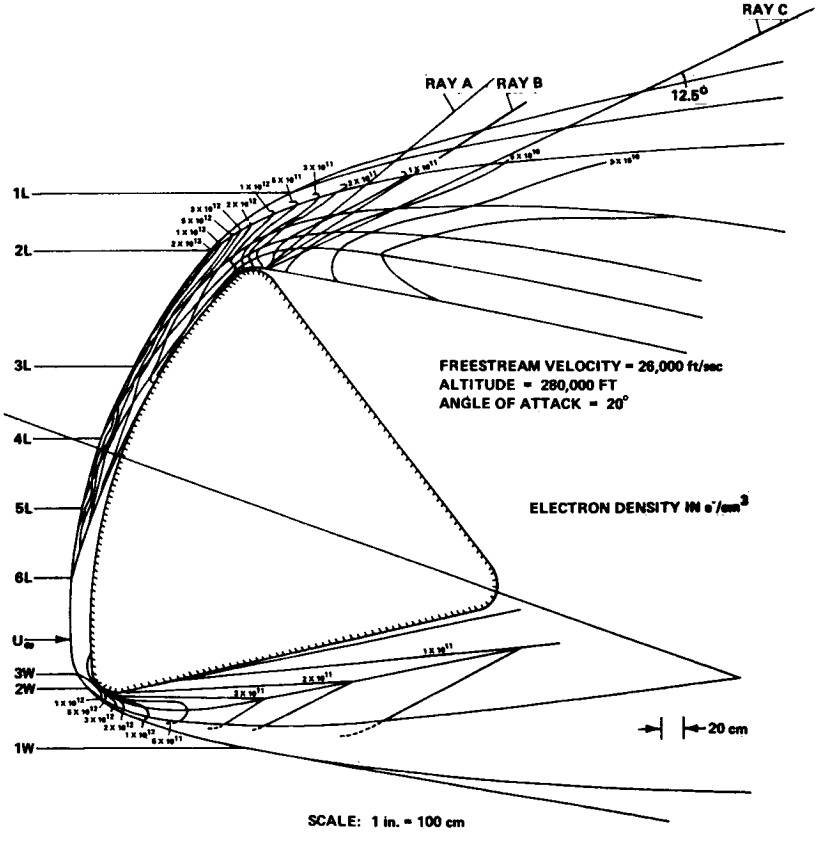

Figure 4.- Electron density distribution in plane of symmetry for Apollo command module.

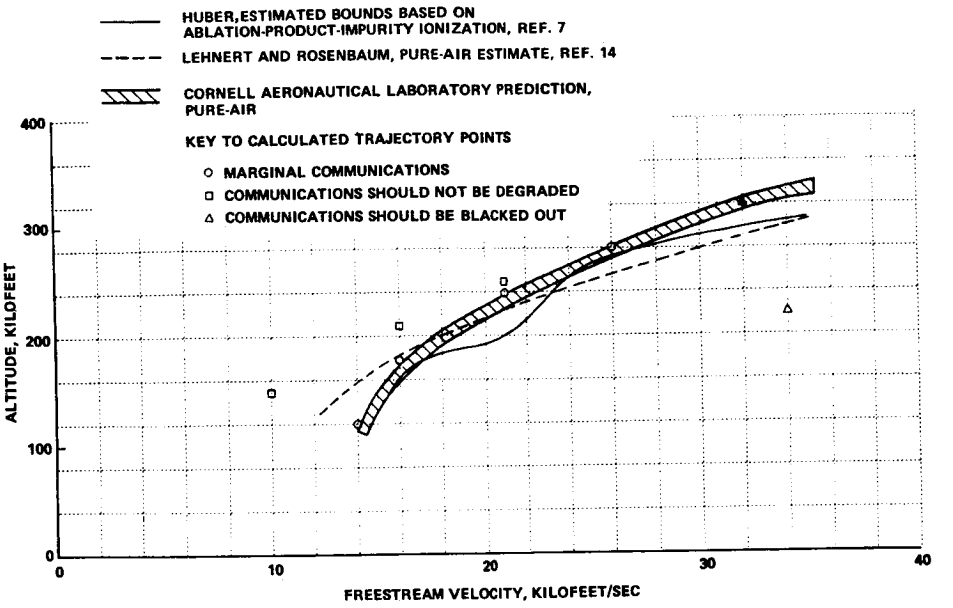

Figure 5.- Predicted blackout bounds for 2.287 GHz communication during Apollo earth-atmosphere entry.

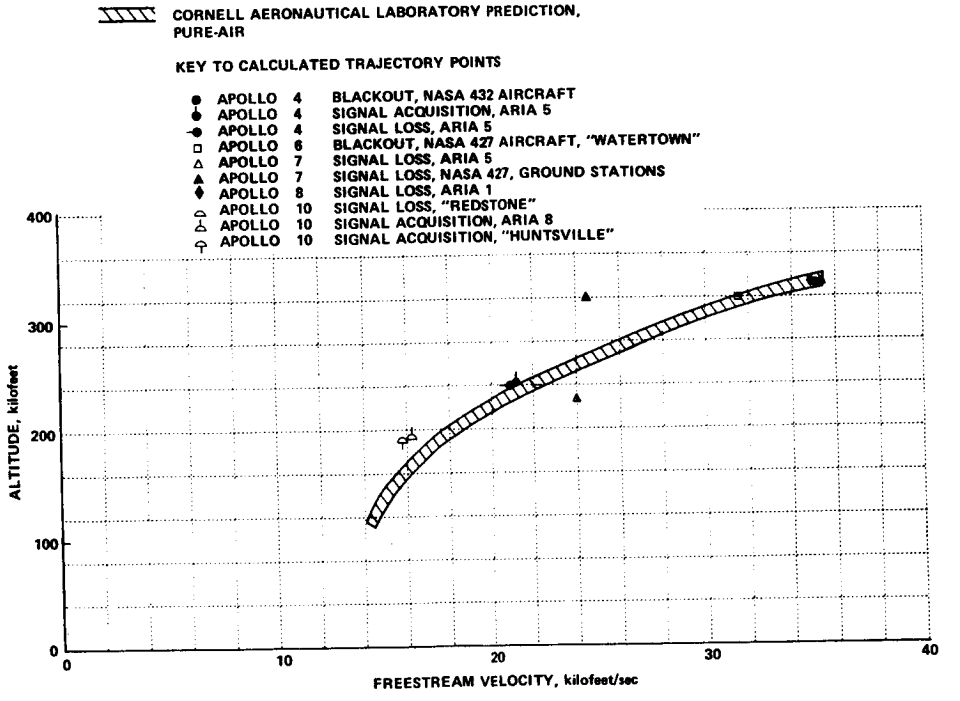

Figure 6.- Comparison between predicted and flight data blackout boundaries.